Iran J Sci Technol Trans Mech Eng (2017) 41:225–232
DOI 10.1007/s40997-016-0057-x

RESEARCH PAPER

Performance Assessment of a Multi-Generation System Based on Organic Rankine Cycle

Moslem Sharifishourabi[1,2] · Tahir Abdul Hussain Ratlamwala[3] · Hamed Alimoradiyan[2] · Ehsan Sadeghizadeh[2]

Received: 12 October 2015 / Accepted: 26 July 2016 / Published online: 17 November 2016

Abstract In this paper, a new multi-generation system is proposed and analyzed through energy and exergy. The new system uses solar power as its energy source and delivers six beneficial productions for the residential sector, such as hotels. These outputs include hot water, electricity, heating, cooling, dry air, and hydrogen production. The effects of some factors such as the inlet and outlet temperature of turbine and ambient temperature on the performances of the system are evaluated. The results show that the energetic COP of the absorption chiller cycle is found to be 60%, whereas the exergetic COP of the absorption system is found to be about 10%. Also, energetic and exergetic efficiency of the organic Rankine cycle is determined to be 8 and 27%, respectively. Moreover, overall energetic and exergetic efficiency of the system is found to be 70 and 53%, respectively.

Keywords Organic Rankine cycle · Multi-generation System · Energy · Exergy · Efficiency

List of symbols

$\dot{E}x$	Exergy rate (kW)
Ex	Specific exergy (kJ/kg)
h	Specific enthalpy (kJ/kg)
$\dot{m}$	Mass flow rate (kg/s)
P	Pressure (kPa)
Tb	Turbine
EG	Electricity generator
S	Specific entropy (kJ/kg-K)
t	Temperature (K)
V	Specific volume (m^3/kg)
abs	Absorber
Evap	Evaporator
EV	Expansion valve
TV	Throttle valve
SG	Steam generator
El	Electrolyzer
LiBr	Lithium bromide
1, 2,…,32	State numbers
d	Destruction
G	Generator
$P\ i$	Pump i
$P\ ii$	Pump ii
$C\ i$	Condenser i
$C\ ii$	Condenser ii
HEX i	Heat exchanger i
HEX ii	Heat exchanger ii
η	Energy efficiency
Ψ	Exergy efficiency

✉ Moslem Sharifishourabi
moslem.sharifishourabi.1@ulaval.ca

[1] Department of Mechanical Engineering, Faculty of Science and Engineering, Université Laval, Québec, QC G1V 0A6, Canada

[2] Department of Mechanical Engineering, Faculty of Engineering, Eastern Mediterranean University, Magusa, Mersin 10, Turkey

[3] Shaheed Zulfikar Ali Bhutto Institute of Science and Technology, Clifton Campus, Karachi, Sindh, Pakistan

1 Introduction

In recent times, environmental risks and energy production issues have prompted nations around the world to begin implementing initiatives that focus on creating and using renewable energy sources. There has also been a global push to reduce the current amount of fossil fuels being used (Ratlamwala and Dincer 2013; Ahmadi et al. 2013). This is

because fossil fuels are known to release lethal pollutants that are extremely harmful to the environment. Therefore, the application of alternate energy sources such as geothermal, solar, hydropower, nuclear energy, and wind energy is an important step for the future (Ahmadi et al. 2013; Khalid et al. 2015; Kaviri et al. 2013). Solar energy, in particular, has become one of the most popular alternative energy sources because it is free and does not harm the environment (Atikol et al. 2013). Today, there are many power plants which are being run using solar energy. When looking into the different ways of creating power with solar energy, there are a variety of techniques. These include solar towers, solar dishes, and parabolic trough solar collectors (PTSCs). PTSCs have been used in large power plants since the 1980s. Nowadays, many thermal solar power plants choose to work with PTSCs (Al-Sulaiman et al. 2012). A PTSC has been selected for this system because it is able to increase the heat transmission at a faster rate.

Many researchers have worked on the multi-generation systems. Suleman et al. (2014) developed a novel multi-generation system that integrated geothermal and solar. Their results showed that the overall exergetic efficiencies of ORC 1 and 2 are 82.3 and 77.1%, respectively, whereas the energetic efficiencies are 38.3 and 23.2%, respectively. Exergetic COP of the absorption cooling cycle was 0.41, while the energetic COP was 0.77. Furthermore, the overall exergetic efficiency of the cycle was 76.4%, and the energetic efficiency of the system was 54.7%. In their study, Ozturk and Dincer (2013) presented a multi-generation system based on solar and studied energy and exergy analyses. The organic Rankine cycle efficiency was found 13.51%, Rankine cycle efficiency was calculated as 40.94%, utilization system efficiency and hydrogen production were determined as 21.30%, and absorption cycle efficiency was found 32.75%. Energy efficiency of the system was determined as 52.71%, while exergy efficiency of the cycle was determined as 57.35%. Absorption, organic Rankine, Rankine, and hydrogen production and utilization cycles had exergy efficiencies of 14.31, 19.62, 44.88, and 20.32%, respectively. Bicer and Dincer (2015) have designed and analyzed an integrated system for syngas, bitumen, electricity, and hydrogen production at the same time with steam-assisted gravity drainage and underground coal gasification. The proposed system highlights the significance of multi-generation systems. In their study, energy efficiencies of components were determined as 75% for UCG process and 50% for Brayton cycle. Exergy and energy efficiencies of the overall system were 17.3 and 19.6%, respectively. Khalid et al. (2015) developed a new renewable system-based multi-generation through energy and exergy analysis. The overall exergy and energy efficiencies of the proposed system, which use solar energy and biomass, were 39.7 and 66.5%, respectively; on the other hand, the exergy and energy efficiencies were 37.6 and 64.5%, respectively, when the system operated with only biomass, while they were 44.3 and 27.3% when the system operated with only solar.

In this study, the solar power plant is integrated with a dryer and an electrolyzer, as well as SEAS, which generates hot water, heat, dry air, cooling, hydrogen, and electricity. This study proposes a new multi-generation system that uses new working fluids involving 58NaCl_42$MgCl_2$ for parabolic trough solar collector cycle, LiBr–water for the single-effect absorption system (SEAS), and R134a for the drying cycle. As previously stated, this system can be used in the future in the residential sector in places such as hotels.

2 System Description

According to Fig. 1, the system consists of five subsystems such as a single-effect absorption system, a parabolic trough solar collector, a dryer, an electrolyzer, and an organic Rankine cycle (the main productions of the system are dry air, heating, cooling, electricity, hot water, and hydrogen). Solar energy was selected as the source of energy for this study. The parabolic trough collector consists of two components such as collector and receiver, and the heat engine is selected to collect the thermal energy of the solar radiation. The 58NaCl_42$MgCl_2$ is selected as a molten salt to use as a working fluid in PTSC cycle. The organic Rankine cycle consists of six components including a heat exchanger, a pump, a turbine, a condenser, and a steam generator. The working fluid which is in ORC should have high temperature to certify an efficient process. The isobutane is selected as the working fluid for ORC due to the high thermal capabilities and easy availability. Moreover, R134a and LiBr–water are selected as working fluids in the dryer cycle and absorption chiller, respectively.

In this system, solar collectors collect the thermal energy from the sun by circulating molten salt throughout the cycle. When the molten salt is processed in the cycle, it attracts the thermal energy from the sun and becomes hot. Once it has captured the heat, the molten salt will disperse a high-temperature transfer to the isobutene, which is the working fluid in the organic Rankine cycle. This process runs the turbine to produce electricity and can eventually create hydrogen production as well. Moreover, the heat can be transferred to the single-effect absorption system by the generator, which can run the SEAS and produce hot water, cooling, and dry air.

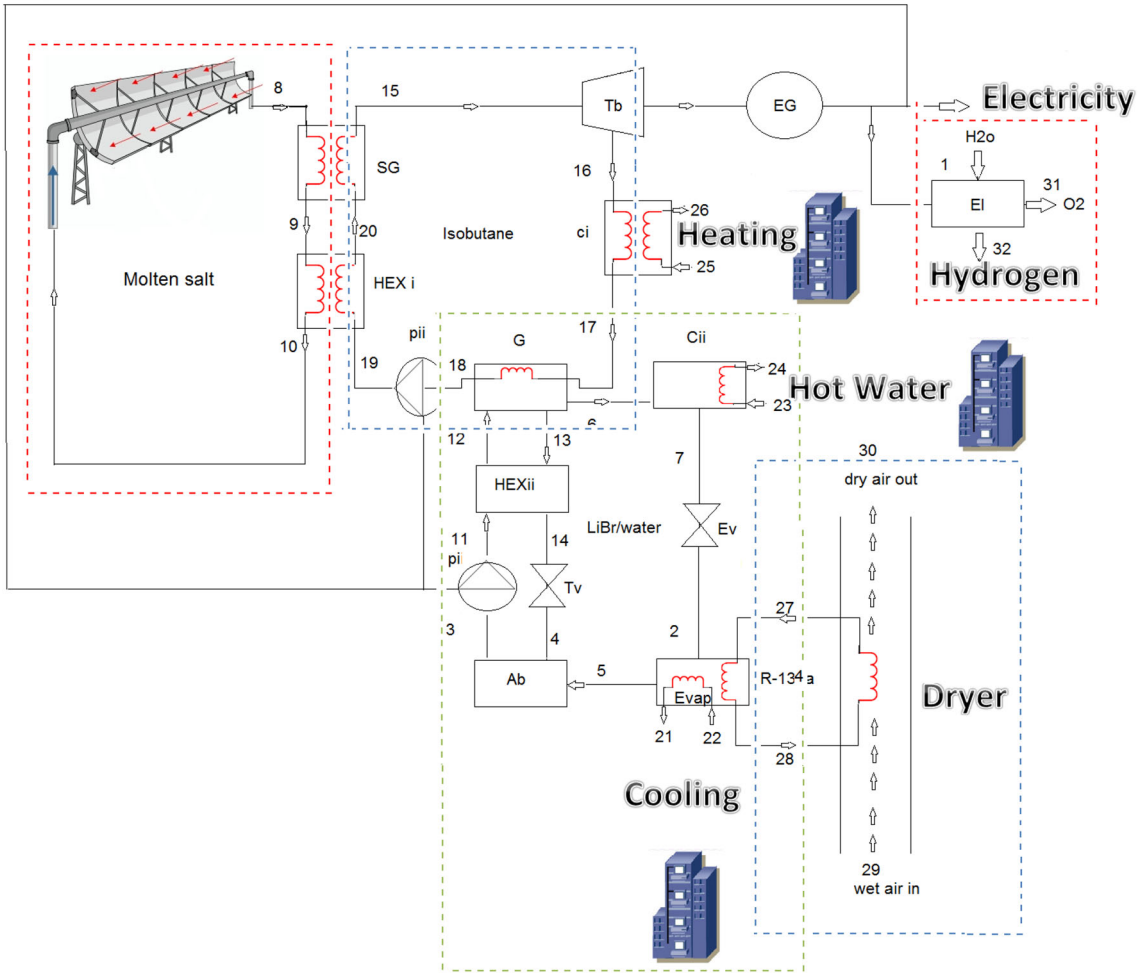

Fig. 1 Schematic diagram of the multi-generation system

3 Thermodynamic Analysis

In this paper, the following assumptions are made:

- Air is treated as an ideal gas.
- The reference environment state has a temperature of $T_0 = 297$ K and a pressure of $P_0 = 101$ kPa.
- The turbine is adiabatic.
- The heat exchangers do not have any heat losses.
- The pressure losses in all heat exchangers and pipelines are negligible.
- Moreover, the solar multi-generation system is supposed to operate in a steady-state condition.

According to Dincer and Rosen (2012), the balanced equations for mass, energy, and exergy are defined for major components. Also, coefficients of performance (COP) are determined for the SEAS.

3.1 Rankin Cycle

3.1.1 Turbine

Mass, energy, and exergy balances for the turbine can be written as follows:

$$\dot{m}_{15} = \dot{m}_{16} \tag{1}$$

$$\dot{m}_{15} h_{15} = \dot{m}_{16} h_{16} + \dot{w}_T \tag{2}$$

$$\dot{m}_{15} ex_{15} = \dot{m}_{16} ex_{16} + \dot{w}_T + \dot{E}xd_T \tag{3}$$

3.1.2 Condenser i

Mass, energy, and exergy of the condenser i can be calculated from:

$$\dot{m}_{16} = \dot{m}_{17} \tag{4}$$

$$\dot{m}_{16}h_{16} + \dot{m}_{25}h_{25} = \dot{m}_{17}h_{17} + \dot{m}_{26}ex_{26} + \dot{Q}_{ci} \quad (5)$$

$$\dot{m}_{16}ex_{16} + \dot{m}_{25}ex_{25} = \dot{m}_{17}ex_{17} + \dot{m}_{26}ex_{26} + \dot{Q}_{ci}\left(1 - \frac{T_0}{T_{ci}}\right) + \dot{E}xd_{ci} \quad (6)$$

3.1.3 Pump ii

Mass, energy, and exergy balances for the pump ii can be written as follows:

$$\dot{m}_{18} = \dot{m}_{19} \quad (7)$$

$$\dot{w}_{pii} = \dot{m}_{18} \times v_{18}(p_{19} - p_{18}) \quad (8)$$

$$\dot{m}_{18}ex_{18} + \dot{w}_{pii} = \dot{m}_{19}ex_{19} + \dot{E}xd_{pii} \quad (9)$$

3.1.4 Heat Exchanger i

Mass, energy, and exergy of the heat exchanger i can be calculated from:

$$\dot{m}_9 + \dot{m}_{19} = \dot{m}_{10} + \dot{m}_{20} \quad (10)$$

$$\dot{m}_{19}h_{19} + \dot{Q}_{HEXi} = \dot{m}_{20}h_{20} \quad (11)$$

$$\dot{m}_9ex_9 + \dot{m}_{19}ex_{19} = \dot{m}_{20}ex_{20} + \dot{m}_{10}ex_{10} + \dot{E}xd_{HEXi} \quad (12)$$

3.1.5 Steam Generator

Mass, energy, and exergy balances for the steam generator can be written as follows:

$$\dot{m}_8 + \dot{m}_{20} = \dot{m}_9 + \dot{m}_{15} \quad (13)$$

$$\dot{m}_{20}h_{20} + \dot{Q}_{SG} = \dot{m}_{15}h_{15} \quad (14)$$

$$\dot{m}_{20}ex_{20} + \dot{Q}_{SG}\left(1 - \frac{T_0}{T_{SG}}\right) = \dot{m}_{15}ex_{15} + \dot{E}xd_{SG} \quad (15)$$

3.1.6 Generator

Mass, energy, and exergy of the generator can be determined from:

$$\dot{m}_{12} = \dot{m}_{13} + \dot{m}_6 \quad (16)$$

$$\dot{m}_{17}h_{17} = \dot{m}_{18}h_{18} + \dot{Q}_G \quad (17)$$

$$\dot{m}_{17}ex_{17} = \dot{m}_{18}ex_{18} + \dot{Q}_G\left(1 - \frac{T_0}{T_G}\right) + \dot{E}xd_G \quad (18)$$

3.2 Absorption Chiller Cycle

3.2.1 Heat Exchanger ii

Mass, energy, and exergy of the heat exchanger ii can be calculated from:

$$\dot{m}_{11} + \dot{m}_{13} = \dot{m}_{12} + \dot{m}_{14} \quad (19)$$

$$\dot{m}_{11}h_{11} + \dot{Q}_{HEXii} = \dot{m}_{12}h_{12} \quad (20)$$

$$\dot{m}_{11}ex_{11} + \dot{m}_{13}ex_{13} + \dot{Q}_{HEXii}\left(1 - \frac{T_0}{T_{HEXii}}\right) = \dot{m}_{12}ex_{12} + \dot{m}_{14}ex_{14} + \dot{E}xd_{HEXii} \quad (21)$$

3.2.2 Condenser ii

Mass, energy, and exergy balances for the condenser ii can be written as follows:

$$\dot{m}_6 = \dot{m}_7 \quad (22)$$

$$\dot{m}_6h_6 = \dot{m}_7h_7 + \dot{Q}_{cii} \quad (23)$$

$$\dot{m}_6ex_6 = \dot{m}_7ex_7 + \dot{Q}_{cii}\left(1 - \frac{T_0}{T_{cii}}\right) + \dot{E}xd_{cii} \quad (24)$$

3.2.3 Pump i

Mass, energy, and exergy of the pump i can be determined from:

$$\dot{m}_3 = \dot{m}_{11} \quad (25)$$

$$\dot{w}_{pi} = \dot{m}_{15}(h_{11} - h_3) \quad (26)$$

$$\dot{m}_3ex_3 + \dot{w}_{pi} = \dot{m}_{11}ex_{11} + \dot{E}xd_{pi} \quad (27)$$

3.2.4 Evaporator

Mass, energy, and exergy balances for the evaporator can be written as follows:

$$\dot{m}_2 = \dot{m}_5 \quad (28)$$

$$\dot{m}_2h_2 + \dot{Q}_{eva} = \dot{m}_5h_5 \quad (29)$$

$$\dot{m}_2ex_2 + \dot{Q}_{eva}\left(\frac{T_0}{T_{eva}} - 1\right) = \dot{m}_5ex_5 + \dot{E}xd_{eva} \quad (30)$$

3.2.5 Absorber

Mass, energy, and exergy of the absorber can be calculated from:

$$\dot{m}_4 + \dot{m}_5 = \dot{m}_3 \quad (31)$$

$$\dot{m}_4h_4 + \dot{m}_5h_5 = \dot{m}_3h_3 + \dot{Q}_{abs} \quad (32)$$

$$\dot{m}_4ex_4 + \dot{m}_5ex_5 = \dot{m}_3ex_3 + \dot{Q}_{abs}\left(1 - \frac{T_0}{T_{abs}}\right) + \dot{E}xd_{abs} \quad (33)$$

3.3 Drying Process

$$\dot{Q}_{Dryer} = \dot{m}_{29} * h_{29} - (\dot{m}_{30} * h_{30} + \dot{m}_{water} * h_{water}) \quad (34)$$

$$\eta_{Dryer} = \frac{\dot{m}_{30} * h_{30}}{\dot{Q}_{Dryer}} \quad (35)$$

3.4 Electrolyzer

$$\dot{m}_{H_2} = \frac{\eta_{elec} * \dot{w}_{net}}{HHV} \quad (36)$$

where η_{elec} is 0.56 and HHV (higher heating value of hydrogen) is 235.15 (kJ/g-mol).

3.5 The Energetic COP of Absorption Chiller

$$COP_{En} = \frac{\dot{Q}_{eva} + \dot{Q}_{Cii}}{\dot{Q}_G + \dot{w}_{Pi}} \quad (37)$$

3.6 The Exergetic COP Absorption Chiller

$$COP_{En} = \frac{\dot{} + \dot{}}{\dot{} + \dot{w}_{Pi}} \quad (38)$$

3.7 The Energetic Efficiency of ORC

$$\eta_{ORC} = \frac{\dot{W}_{net}}{\dot{Q}_{in}} \quad (39)$$

3.8 The Exergetic Efficiency of ORC

$$\Psi_{ORC} = \frac{\dot{W}_{net}}{\dot{}} \quad (40)$$

4 Results and Discussion

Comprehensive energy and exergy analysis of the system has been done, and the results are given in Tables 1 and 2. A comparative study was carried out using results found in similar studies. The effects of energy and exergy efficiency of the components were compared to other similar studies

Table 1 Comparison of the exergy destruction of the current study with previous study

Component	Current study (kW)	Previous study (kW) (Ozturk 2012)
Boiler	0.9	564.1
Absorber	48.79	98.25
Turbine	18.29	259
Condenser ii	2.5	19
Pump ii	0.16	114
Pump i	0.51	45

Table 2 Outputs of the system

Parameter	Value
Overall energy efficiency	70%
Overall exergy efficiency	53%
Energetic efficiency of ORC	8%
Exergetic efficiency of ORC	27%
Energetic COP	60%
Exergetic COP	10%
Turbine work	157.8 kW
Cooling effect	486.9 kW
Heating effect	632.1
Hydrogen production	0.0003

(Islam et al. 2015; Ozlu and Dincer 2015; Ozturk 2012), and respectable agreements are created. In particular, the exergy destruction of some components is compared with the Ozturk system (2012), and the results are shown in the Table 3.

As it is shown in the Table 1, the exergy destruction of the components is less than previous study. All modelings have been carried out by Engineering Equation Solver (EES) software.

4.1 Effect of Turbine Inlet Pressure on Efficiencies

The effects of turbine inlet pressure on the efficiencies of the system are shown in Fig. 2. It can be seen that by growing the inlet pressure of turbine both the overall and ORC efficiencies are falling. When the turbine inlet pressure is increased from 2500 to 5000 (kPa), the overall energetic and exergetic efficiency is decreased from 59 to 64% and the overall exergy efficiency of the multi-generation cycle increased from 69 to 66% and from 52 to 34%, respectively. In addition, the energetic and exergetic efficiency of ORC is decreased from 7 to 4% and from 27 to 24%, respectively. This is because a rise in the turbine inlet pressure produces additional work for the turbine pump.

4.2 Effect of Turbine Inlet Temperature on ORC Efficiencies

The influence of the turbine inlet temperature on the energetic and exergetic efficiency of ORC is presented in Fig. 3. It can be seen that by increasing the inlet temperature of the ORC turbine, the energy efficiency increases quickly while the exergy efficiency does as well, but at a much slower rate. By increasing the inlet temperature of turbine from 530 to 630 K, the energetic and exergetic efficiency of ORC increases from 4 to

Table 3 Thermodynamic properties of the system at each state point

Point	t (K)	P (kPa)	$\dot{m}$ (kg/s)	h (kJ/kg)	S (kJ/kg.K)	Exergy rate (kW)
0	297	101		71.77	5.708	
1	298	101	1	104.2	0.3648	
2	280.1	1	0.2	79.03	0.1056	1671
3	300	1	2.5	59.24	0.1747	1631
4	308.6	1	2.3	103	0.2061	1665
5	280.2	1	0.2	2513	8.974	1472
6	320	5.5	0.2	2587	8.433	1706
7	292	5.5	0.2	79.03	0.2798	1619
8	973	101.3	10	275.5	0.3281	1801
9	910.1	101.3	10	207.6	0.2558	1755
10	795.3	101.3	10	83.58	0.11	1674
11	300.1	5.5	2.5	59.45	0.1754	1631
12	310.1	5.5	2.5	80.32	0.244	1631
13	325	5.5	2.3	188.5	0.3086	1720
14	313.6	5.5	2.3	103	0.2378	1656
15	540	2500	2.5	1112	3.311	1752
16	510	850	2.5	1049	3.336	1681
17	490	850	2.5	996.3	3.231	1660
18	330	850	2.5	341.2	1.464	1530
19	331	2500	2.5	343.9	1.463	1533
20	440	2500	2.5	840	2.755	1645
21	283	101.3	31.08	283.4	5.643	230.7
22	298	101.3	31.08	298.4	5.695	230.4
23	298	101.3	4	104.2	0.3648	1619
24	328	101.3	4	229.6	0.7657	1626
25	293	101.3	5	83.3	0.294	1619
26	317	101.3	5	183.6	0.6231	1622
27	233	50	31.08	225.8	0.9704	1561
28	233	50	31.08	225.8	0.9704	1561
29	308	101	5.397	128.4	5.764	215.18
30	288	101	5.397	41.69	5.759	−245.2
32	299	101	0.003	12.19	64.82	−5.187

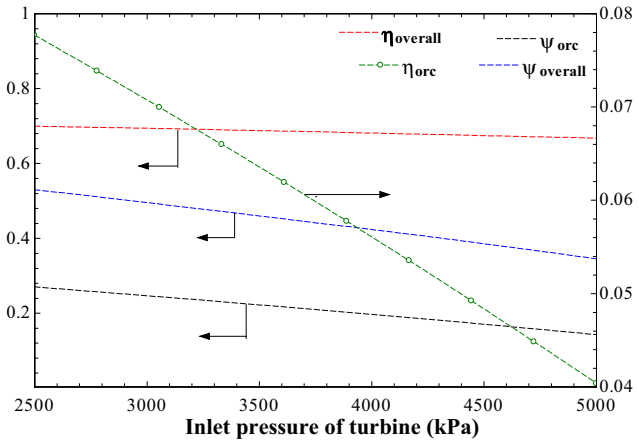

Fig. 2 Effect of turbine inlet pressure on the efficiencies

31% and from 15 to 92%, respectively. This is due to increase in the inlet enthalpy of turbine and turbine work.

4.3 Effect of the turbine inlet temperature on the turbine work and hydrogen production

Figure 4 shows that an increase in the inlet temperature of the turbine causes a rise in both the turbine work and hydrogen production rate. It can be seen that by increasing the ORC turbine inlet temperature from 530 to 630 (K), the turbine work increases from 87 to 825 kW and also hydrogen production increases from 0.00015 to 0.0016 kg/s because of the increase in the inlet temperature of turbine case an increase in the inlet enthalpy of turbine.

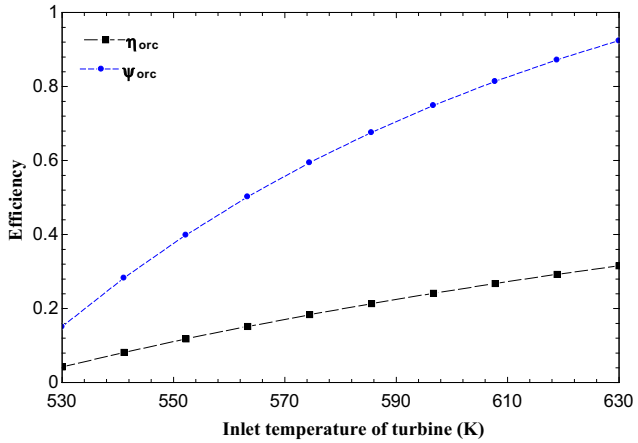

Fig. 3 Effect of inlet temperature of turbine on the ORC efficiencies

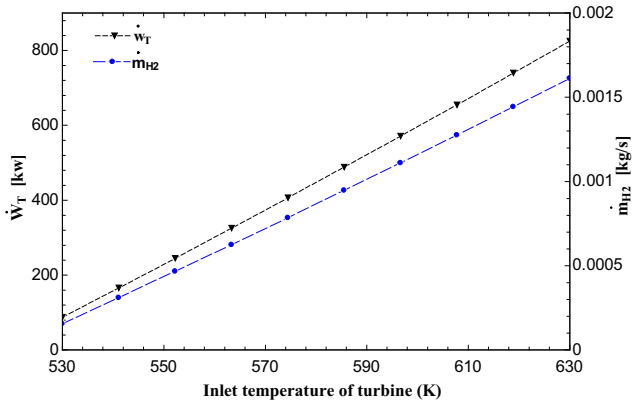

Fig. 4 Effect of the turbine inlet temperature on the turbine work and hydrogen production

4.4 Effect of the Turbine Outlet Temperature on the ORC Efficiencies

Figure 5 shows that an increase in the outlet temperature of the turbine causes a decrease in the both efficiencies. It is obvious that when the outlet temperature is increased from 460 to 520 (K), the ORC energy efficiency decreased from 24 to 4%. Also, by raising the turbine outlet temperature, the ORC exergy efficiency is decreased from 84% to nearly 14%. It is due to a growth in the exergy destruction of the turbine.

4.5 Effect of Environment Temperature on the Efficiencies

The effects of ambient temperature on the efficiencies are shown in Fig. 6. It can be seen that there is, in fact, no direct effect on the energy efficiency of the ORC and energetic COP because they do not consider heat losses. On the other hand, the rise in the ambient temperature causes a growth in both the exergetic COP and exergetic efficiency

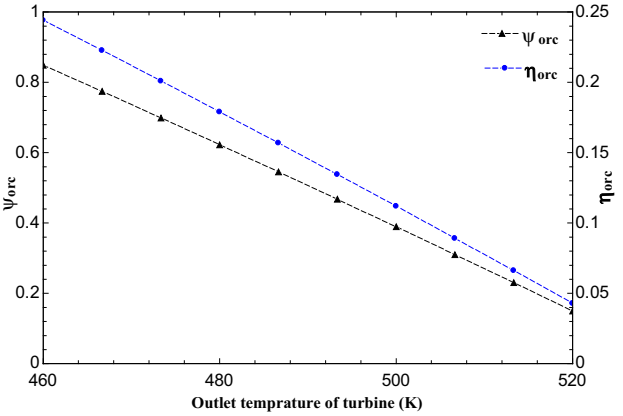

Fig. 5 Effect of the turbine outlet temperature on the ORC efficiencies

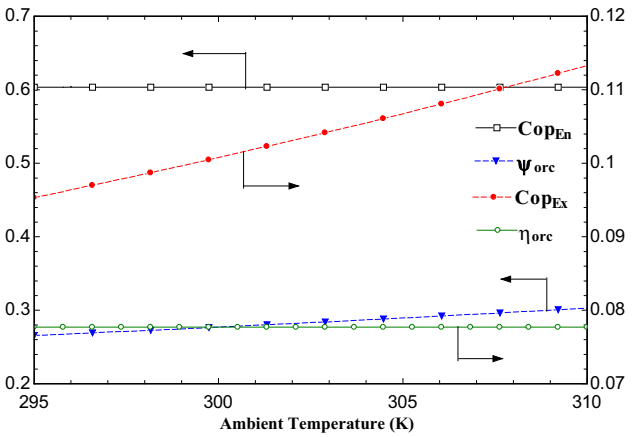

Fig. 6 Effect of ambient temperature on the efficiencies

of ORC. This is due to decreased temperature difference between ambient and system.

4.6 Efficiencies of Subsystems

The Efficiencies of Subsystems are shown in Fig. 7. The energetic efficiency of dryer, energetic efficiency of electrolyzer, exergetic efficiency of ORC, and energetic COP of chiller are determined to be 48.71, 56, 27, and 60%, respectively.

5 Conclusions

The new multi-generation system, analyzed in this report, is capable of supplying energy to residential sectors such as hotels. It is able to provide the production of heating, cooling, hydrogen hot water, dry air, and electricity. The results of the study show that the energetic COP of single-effect absorption system is 60% while the exergetic COP is 10%. Also, the overall energy efficiency is found to be

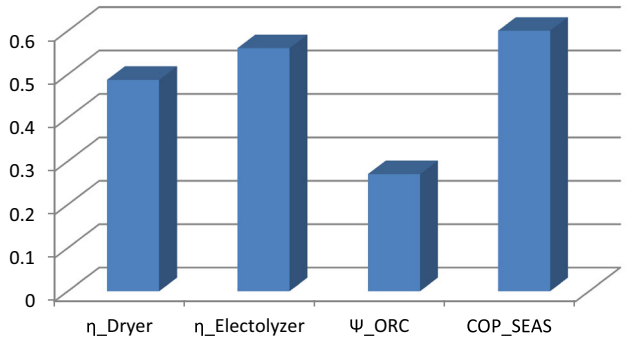

Fig. 7 Efficiency of subsystems

70%, while the overall exergy efficiency is determined to be about 53%. Moreover, energy efficiency of the ORC is calculated to be 8%, and exergy efficiency of the ORC is determined to be 27%.

The exergy results, in particular, identify the generator as the component with the greatest exergy destruction rate, meaning that it is the main source of irreversibility. However, the system is inline with the renewable energy initiatives being implemented by the global community and is an important system for the future.

References

Ahmadi P, Dincer I, Rosen MA (2013a) Development and assessment of an integrated biomass-based multi-generation energy system. Energy 1(56):155–166

Ahmadi P, Dincer I, Rosen MA (2013b) Performance assessment and optimization of a novel integrated multigeneration system for residential buildings. Energy Build 31(67):568–578

Al-Sulaiman FA, Hamdullahpur F, Dincer I (2012) Performance assessment of a novel system using parabolic trough solar collectors for combined cooling, heating, and power production. Renew Energy 48:161–172

Atikol U, Abbasoglu S, Nowzari R (2013) A feasibility integrated approach in the promotion of solar house design. Int J Energy Res 37(5):378–388

Bicer Yusuf, Dincer Ibrahim (2015) Development of a multigeneration system with underground coal gasification integrated to bitumen extraction applications for oil sands. Energy Convers Manag 106:235–248

Dincer I, Rosen MA (2012) Exergy: energy, environment and sustainable development. Newnes, Oxford

Islam S, Dincer I, Yilbas BS (2015) Energetic and exergetic performance analyses of a solar energy-based integrated system for multigeneration including thermoelectric generators. Energy 93:1246–1258

Kaviri AG, Jafar MM, Tholudin ML, Sharifishourabi G (2013) Modelling and exergoeconomic based design optimisation of combined power plants. Int J Exergy 13(2):141–158

Khalid Farrukh, Dincer Ibrahim, Rosen Marc A (2015) Energy and exergy analyses of a solar-biomass integrated cycle for multigeneration. Sol Energy 112:290–299

Ozlu Sinan, Dincer Ibrahim (2015) Development and analysis of a solar and wind energy based multigeneration system. Sol Energy 122:1279–1295

Ozturk M (2012) Thermodynamics assessment of the multi-generation energy production systems. INTECH Open Access Publisher, Rijeka

Ozturk Murat, Dincer Ibrahim (2013) Thermodynamic analysis of a solar-based multi-generation system with hydrogen production. Appl Therm Eng 51(1):1235–1244

Ratlamwala TA, Dincer I (2013) Performance assessment of solar-based integrated Cu–Cl systems for hydrogen production. Sol Energy 30(95):345–356

Suleman F, Dincer I, Agelin-Chaab M (2014) Development of an integrated renewable energy system for multigeneration. Energy 78:196–204